Bending losses of incoherent light in circular hollow waveguides

Mitsunori Saito, Yuji Matsuura, Masashi Kawamura, and Mitsunobu Miyagi

Department of Electrical Communications, Faculty of Engineering, Tohoku University, Sendai 980, Japan

Received October 9, 1989; accepted May 15, 1990

Optical losses of incoherent light in bent hollow waveguides are analyzed theoretically. The analysis is based on geometrical optics and provides a much simpler and efficient calculation method than the conventional ray-tracing method. By comparing theoretical and experimental results, it is demonstrated that the present calculation method gives precise evaluations for the bending losses.

INTRODUCTION

Flexible light transmission is desired strongly in infrared technology such as high-power laser delivery, thermometry, and spectroscopy. Since conventional silica-based fibers are not available in the mid- and far-infrared regions, many types of hollow waveguides as well as nonoxide fibers have been developed in the last decade.[1–4] If compared with solid-core fibers, hollow waveguides are more sensitive to bending,[4–6] although they are superior to the fibers in some respects. Therefore the bending loss is one of the most important features to characterize the hollow waveguides.

There have been many theoretical studies on the optical properties of bent waveguides.[7–10] However, most of the conventional studies were concerned only with the coherent light transmission of several lower-order modes in the waveguides, and a bending loss of diffusive nonlaser light has not been investigated well so far. The transmission properties of such an incoherent light of extreme multimodes can be analyzed in terms of geometrical optics. Although ray tracing is often achieved in geometrical optics,[11,12] it is inherently time consuming and is not free from statistical errors. For some simple cases, e.g., a straight fiber and a weakly guiding fiber, algebraic expressions for the optical loss have been derived based on ray optics in order to avoid tracing numerous rays one by one.[13–15] To our knowledge, however, such a simple expression has not been derived yet for the bending hollow waveguides, since it has been believed that the complicated behavior of skew rays should be considered in this case.

In this paper we prove that the average loss of skew rays can be evaluated without taking into account skewness of hollow waveguides in some cases. Then we derive a simple equation to evaluate the loss of incoherent light in a bent hollow waveguide. Finally, we calculate numerically the bending losses of three types of hollow waveguide and compare them with the experimental results.

THEORY

Let us consider a circular hollow waveguide, shown in Fig. 1. We assume an inner diameter $2T$, a length l, and a bending radius R of the waveguide to be $\sim$1 mm, $\sim$1 m, and $\gtrsim$0.3 m, respectively. We also assume that the incident rays are of an axially symmetrical distribution with the incident angle θ_0 of the order of 10^{-1} rad. These values have been chosen to meet the conditions of our experiment and many practical applications of the waveguide.

A ray traveling in the waveguide can be expressed with position parameters (Θ, r, ϕ) and direction parameters $(\Theta, \theta, \varphi)$. If the ray leaves the entrance of the waveguide $(\Theta = 0)$ at a position $(0, r_0, \phi_0)$ toward a direction $(0, \theta_0, \varphi_0)$, an angle Θ_1 at which the ray first comes across the waveguide wall is obtained by solving a quartic equation[11]:

$$A_1 \tan^4 \frac{\Theta_1}{2} + A_2 \tan^3 \frac{\Theta_1}{2} + A_3 \tan^2 \frac{\Theta_1}{2} + A_4 \tan \frac{\Theta_1}{2} + A_5 = 0, \quad (1)$$

where A_i's $(i = 1, 2, 3, 4, 5)$ are

$$\begin{aligned}
A_1 &= (4R^2 + 4Rr_0 \cos \phi_0 + {r_0}^2 - T^2)\cos^2 \theta_0, \\
A_2 &= 2[(2R^2 - T^2)\cos \varphi_0 + Rr_0 \cos(\varphi_0 + \phi_0) \\
&\quad - {r_0}^2 \sin \phi_0 \sin(\varphi_0 - \phi_0)]\sin 2\theta_0, \\
A_3 &= 4\{[R \sin \varphi_0 + r_0 \sin(\varphi_0 - \phi_0)]^2 + (R^2 - T^2)\cos^2 \varphi_0\} \\
&\quad \times \sin^2 \theta_0 + 2(2Rr_0 \cos \phi_0 + {r_0}^2 \cos 2\phi_0 + T^2)\cos^2 \theta_0, \\
A_4 &= 2[Rr_0 \cos(\varphi_0 - \phi_0) + {r_0}^2 \sin \phi_0 \sin(\varphi_0 - \phi_0) \\
&\quad + T^2 \cos \varphi_0]\sin 2\theta_0, \\
A_5 &= ({r_0}^2 - T^2)\cos^2 \theta_0. \qquad (2)
\end{aligned}$$

Since the relations

$$r_0/R \leqq T/R \lesssim 10^{-3}, \qquad \theta_0 \approx 10^{-1}, \qquad \Theta_1 \approx T/(R\theta_0) \lesssim 10^{-2} \quad (3)$$

hold under the assumptions mentioned earlier, the solution Θ_1 of Eq. (1) is approximately expressed as

$$\Theta_1 \fallingdotseq T/(R\theta_0)\{[1 - (r_0/T)^2 \sin^2(\varphi_0 - \phi_0)]^{1/2} - (r_0/T)\cos(\varphi_0 - \phi_0)\}. \quad (4)$$

0740-3232/90/112063-06$02.00

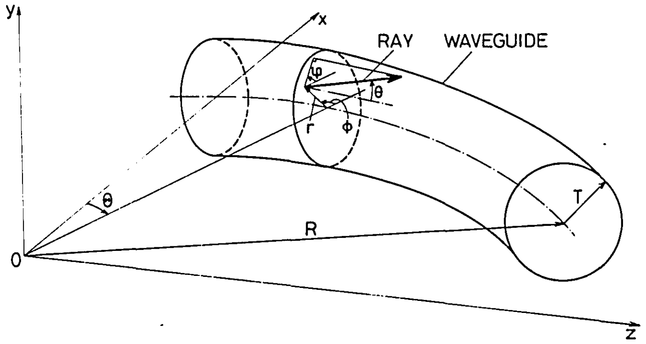

Fig. 1. Model of a bent hollow waveguide.

At the first reflection point ($\Theta = \Theta_1$), the ray is reflected toward the direction of ($\Theta_1, \theta_1, \varphi_1$). After some geometrical consideration, the angle θ_1 turns out to be

$$\theta_1 = \arccos(\cos\theta_0 \cos\Theta_1 - \sin\theta_0 \cos\varphi_0 \sin\Theta_1) \fallingdotseq \theta_0 + \Theta_1 \cos\varphi_0. \quad (5)$$

In a similar way, we can trace the ray that travels between the $(i-1)$th and the ith reflection points. Let the position and the direction of the ray be ($\Theta_{i-1}, T, \phi_{i-1}$) and ($\Theta_{i-1}, \theta_{i-1}, \varphi_{i-1}$) at the $(i-1)$th reflection point. Then the parameters at the ith reflection point become

$$\Theta_i \fallingdotseq \Theta_{i-1} - [2T/(R\theta_{i-1})]\cos(\varphi_{i-1} - \phi_{i-1}), \quad (6)$$

$$\theta_i = \arccos[\cos\theta_{i-1}\cos(\Theta_i - \Theta_{i-1}) - \sin\theta_{i-1}\cos\varphi_{i-1} \times \sin(\Theta_i - \Theta_{i-1})] \fallingdotseq \theta_{i-1}, \quad (7)$$

$$\phi_i = \arctan\frac{(R + T\cos\phi_{i-1})\cos\theta_{i-1} - R\cos\theta_i}{(R + T\cos\phi_{i-1})\sin\theta_{i-1}\sin\varphi_{i-1}\sin(\Theta_i - \Theta_{i-1}) + T\sin\phi_{i-1}\cos\theta_i} \fallingdotseq 2\varphi_{i-1} - \phi_{i-1} - \pi, \quad (8)$$

$$\varphi_i = \phi_i + \arcsin\frac{\sin\phi_i[\cos\theta_i\cos(\Theta_i - \Theta_{i-1}) - \cos\theta_{i-1}]/\sin(\Theta_i - \Theta_{i-1}) + \sin\theta_{i-1}\sin\varphi_{i-1}\cos\phi_i}{\sin\theta_i} \fallingdotseq -\varphi_{i-1} + 2\phi_i + \pi. \quad (9)$$

From Eqs. (6)–(9) we have

$$\theta_i \fallingdotseq \theta_{i-1} \fallingdotseq \cdots \fallingdotseq \theta_1, \quad (10)$$

$$\varphi_i - \phi_i \fallingdotseq \varphi_{i-1} - \phi_{i-1} \fallingdotseq \cdots \fallingdotseq \varphi_1 - \phi_1, \quad (11)$$

$$\Theta_i - \Theta_{i-1} \fallingdotseq -[2T/(R\theta_{i-1})]\cos(\varphi_{i-1} - \phi_{i-1}) \fallingdotseq \cdots \fallingdotseq -[2T/(R\theta_1)]\cos(\varphi_1 - \phi_1). \quad (12)$$

Using Eqs. (10)–(12) and the relations $\theta_{i-1} \ll 1$ and $\Theta_i - \Theta_{i-1} \ll 1$, we evaluate a reflection angle Ψ_i (Fig. 2) at the ith reflection point by geometrical consideration:

$$\Psi_i = \arccos[\sin\theta_{i-1}\cos\varphi_{i-1}\cos\phi_i\cos(\Theta_i - \Theta_{i-1}) + \sin\theta_{i-1}\sin\varphi_{i-1}\sin\phi_i + \cos\theta_{i-1}\cos\phi_i\sin(\Theta_i - \Theta_{i-1})] \fallingdotseq \pi/2 + \theta_i\cos(\varphi_i - \phi_i) \fallingdotseq \pi/2 + \theta_1\cos(\varphi_1 - \phi_1). \quad (13)$$

Note that relations (3) are the only assumptions that are used for the approximations in the derivations of Eqs. (4)–(13).

Next we calculate a reflectivity at the waveguide wall. As shown in Fig. 2, the inner surface of the hollow waveguide is often coated with a dielectric thin film so as to enhance the reflectivity.[4] Let the wavelength of light be λ, the film thickness be d, and the refractive indices of the waveguide material and the film be $n - j\kappa$ and n_F, respectively. In a previous paper, we derived exact expressions of the power reflectivities for p and s polarizations, R_p and R_s, on such a dielectric-coated material by taking into account the surface roughness σ.[15] If the incident angle Ψ is close to $\pi/2$, which is usually the case in low-loss waveguides, we can approximate Eq. (A12) of Ref. 15 as

$$R_p = |r_p|^2 \fallingdotseq 1 - [4n_F^2(n_F^2 - 1)^{-1/2}(1 - B_p^2)/(1 - 2B_p\cos\gamma_p + B_p^2)](\pi/2 - \Psi), \quad (14)$$

$$R_s = |r_s|^2 \fallingdotseq 1 - [4(n_F^2 - 1)^{-1/2}(1 - B_s^2)/(1 - 2B_s\cos\gamma_s + B_s^2)](\pi/2 - \Psi), \quad (15)$$

where the coefficients B_p and B_s are defined as

$$B_p = \left\{\frac{[(n^2 - \kappa^2)(n_F^2 - 1)^{1/2} - n_F^2\xi^{1/2}]^2 + [2n\kappa(n_F^2 - 1)^{1/2} - n_F^2\eta^{1/2}]^2}{[(n^2 - \kappa^2)(n_F^2 - 1)^{1/2} + n_F^2\xi^{1/2}]^2 + [2n\kappa(n_F^2 - 1)^{1/2} + n_F^2\eta^{1/2}]^2}\right\}^{1/2} \exp[-8\pi^2\sigma^2(n_F^2 - 1)/\lambda^2], \quad (16)$$

$$B_s = \left\{\frac{(n_F^2 - 1) - 2[(n_F^2 - 1)\xi]^{1/2} - (\xi - \eta)}{(n_F^2 - 1) + 2[(n_F^2 - 1)\xi]^{1/2} - (\xi - \eta)}\right\}^{1/2} \exp[-8\pi^2\sigma^2(n_F^2 - 1)/\lambda^2], \quad (17)$$

with

$$\xi = \{[(n^2 - \kappa^2 - 1)^2 + (2n\kappa)^2]^{1/2} + (n^2 - \kappa^2 - 1)\}/2,$$
$$\eta = \{[(n^2 - \kappa^2 - 1)^2 + (2n\kappa)^2]^{1/2} - (n^2 - \kappa^2 - 1)\}/2, \quad (18)$$

and γ_p and γ_s are defined as

$$\gamma_p = \arctan\frac{2(n_F^2 - 1)^{1/2}[(n^2 - \kappa^2)\eta^{1/2} - 2n\kappa\xi^{1/2}]}{(n^2 + \kappa^2)^2(n_F^2 - 1)/n_F^2 - n_F^2(\xi + \eta)} - \frac{4\pi d(n_F^2 - 1)^{1/2}}{\lambda}, \quad (19)$$

$$\gamma_s = \arctan\frac{2[(n_F^2 - 1)\eta]^{1/2}}{(n_F^2 - 1) - (\xi + \eta)} - \frac{4\pi d(n_F^2 - 1)^{1/2}}{\lambda} + \pi. \quad (20)$$

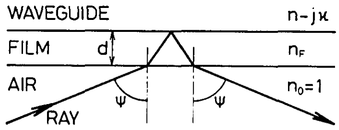

Fig. 2. Reflection at the inner surface of the waveguide coated with a thin film. The surface is assumed to be flat (not curved) since a diameter $2T$ of the waveguide is much larger than the wavelength λ of the light ($T/\lambda \approx 10^2$).

Since rays of random polarization are considered here and the rays are reflected at a variety of angles at the boundary as they spiral down the waveguide, we use the average reflectivity[15]

$$R_A(\Psi) = (R_p + R_s)/2 \fallingdotseq 1 - C(\pi/2 - \Psi), \tag{21}$$

with

$$C = \frac{2}{(n_F^2 - 1)^{1/2}} \times \left[\frac{n_F^2(1 - B_p^2)}{1 - 2B_p \cos\gamma_p + B_p^2} + \frac{1 - B_s^2}{1 - 2B_s \cos\gamma_s + B_s^2}\right] \tag{22}$$

in this calculation.

Finally, we evaluate the attenuation of light in the waveguide. If a ray experiences reflections of m times and loses a power ΔI while it advances a distance of Δl along the waveguide, then the relations

$$\Delta l = R\Theta_m = R\sum_{i=1}^{m}(\Theta_i - \Theta_{i-1}) \fallingdotseq R\sum_{i=1}^{m}[-2T\cos(\varphi_1 - \phi_1)/(R\theta_1)] = -2mT\cos(\varphi_1 - \phi_1)/\theta_1, \tag{23}$$

$$\Delta I/I_0 = \sum_{i=1}^{m}[1 - R_A(\Psi_i)] \fallingdotseq \sum_{i=1}^{m}C(\pi/2 - \Psi_i) \fallingdotseq \sum_{i=1}^{m}C[-\theta_1\cos(\varphi_1 - \phi_1)] = -mC\theta_1\cos(\varphi_1 - \phi_1) \tag{24}$$

hold, where I_0 denotes the initial light intensity and Eqs. (12), (13), and (21) are used in the derivation. From Eqs. (4), (5), (23), and (24), we have

$$(\Delta I/I_0)/\Delta l \fallingdotseq C\theta_1^2/(2T) \fallingdotseq \frac{C}{2T}\left(\theta_0 + \frac{T\cos\varphi_0}{R\theta_0}\left\{\left[1 - \left(\frac{r_0}{T}\right)^2\sin^2(\varphi_0 - \phi_0)\right]^{1/2} - \left(\frac{r_0}{T}\right)\cos(\varphi_0 - \phi_0)\right\}\right)^2. \tag{25}$$

Now let us consider a group of rays that have the same initial values of r_0 and θ_0 but various values of ϕ_0 and φ_0. A total power $P(r_0, \theta_0)$ of these rays and its attenuation ΔP are related to I_0 and ΔI as

$$\Delta P/P(r_0, \theta_0) = \int_0^{2\pi}\int_0^{2\pi}\Delta I \mathrm{d}\phi_0 \mathrm{d}\varphi_0 \bigg/ \int_0^{2\pi}\int_0^{2\pi} I_0 \mathrm{d}\phi_0 \mathrm{d}\varphi_0. \tag{26}$$

In Eq. (26) I_0 does not depend on ϕ_0 and φ_0 since an axially symmetrical power distribution is assumed here. Therefore Eq. (26) reduces to

$$\Delta P/P(r_0, \theta_0) = \int_0^{2\pi}\int_0^{2\pi}(\Delta I/I_0)\mathrm{d}\phi_0 \mathrm{d}\varphi_0 \bigg/ \int_0^{2\pi}\int_0^{2\pi}\mathrm{d}\phi_0 \mathrm{d}\varphi_0. \tag{27}$$

From Eqs. (25) and (27), we can evaluate a power attenuation constant 2α for the group of rays with initial parameters (r_0, θ_0):

$$2\alpha = [\Delta P/P(r_0, \theta_0)]/\Delta l = \int_0^{2\pi}\int_0^{2\pi}[(\Delta I/I_0)/\Delta l]\mathrm{d}\phi_0 \mathrm{d}\varphi_0 \bigg/ \int_0^{2\pi}\int_0^{2\pi}\mathrm{d}\phi_0 \mathrm{d}\varphi_0 = C\theta_0^2/(2T)[1 + T^2/(2R^2\theta_0^4)]. \tag{28}$$

Note that 2α is dependent on θ_0 but not on r_0.

If the light with a directional distribution (far-field pattern) of $p(\theta_0)$ is launched into the waveguide of length l, the attenuation L(dB) of the light intensity becomes

$$L = -10\log\left\{\int_0^{\pi/2} p(\theta_0)\sin\theta_0 \exp[-2\alpha(\theta_0)l]\mathrm{d}\theta_0 \bigg/ \int_0^{\pi/2} p(\theta_0)\sin\theta_0 \mathrm{d}\theta_0\right\}, \tag{29}$$

where the term $\sin\theta_0$ comes from the consideration of a solid angle.[15] Using Eq. (29) with Eq. (28), we can numerically calculate the loss of the bent waveguide.

THEORETICAL AND EXPERIMENTAL RESULTS

Bending losses were measured for three types of hollow waveguide, a nickel tube of 1.5-mm inner diameter with a germanium coating of 0.4 μm thick on its inner surface (Hitachi Cable Ltd.), a nickel tube of 1.6-mm inner diameter without coating, and a silica glass tube of 1.0-mm inner diameter (EOTec Corporation). All these waveguides are 1 m in length. Since the details of the experiment are reported in Refs. 15 and 16, only the results are described here.

Figure 3 shows the attenuation spectra of the incoherent light transmitted through the above waveguides. The waveguides were excited by an incoherent Gaussian beam with FWHM of 6 deg (for the germanium-coated and uncoated nickel tubes) or 5 deg (for the silica tube). Ups and downs in the spectra of the germanium-coated nickel tube, which are not seen in the spectra of the uncoated nickel tube, originate from the optical interference in the germanium film. The optical loss of the silica glass tube decreases near the wavelength of 8 μm at which the real part of the refractive index of silica glass becomes less than unity.

The attenuations of the above-mentioned three waveguides were numerically evaluated by using the refractive index data in Ref. 17. A roughness σ of the inner surface of the waveguide was assumed to be 0.06 μm,[15] and a Gaussian function with FWHM of 5 or 6 deg was used for $p(\theta_0)$. Figure 4 exemplifies the calculated attenuation spectra together with the measured spectra for the germanium-coated nickel waveguide.

Figure 5 shows the dependence of the attenuation on a bending radius. Both in the experiment and in theory, the attenuation increases almost linearly with the curvature $1/R$. The theoretical values coincide well with the measured values in the wavelength region in which the attenuation becomes low, i.e., 6 and 8–10 μm in the germanium-coated nickel waveguide and 8–9 μm in the silica waveguide (see Figs. 3 and 5).

DISCUSSION

Generally optical loss depends on the skewness of the ray, and hence numerous rays of various skewnesses should be

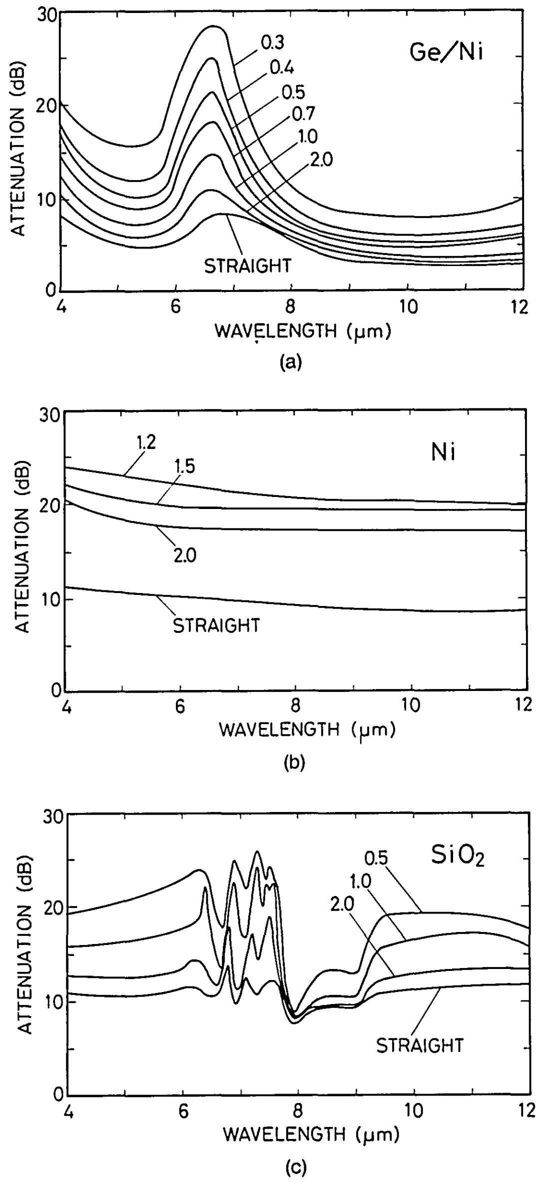

Fig. 3. Attenuation of incoherent light transmitted by three types of hollow waveguide 1 m in length: (a) germanium-coated nickel tube, (b) uncoated nickel tube, (c) silica glass tube. Numbers beside the curves indicate the bending radius R in meters.

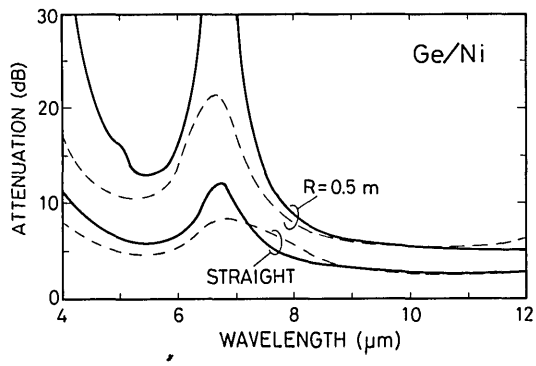

Fig. 4. Calculated (solid curves) and measured (dashed curves) attenuation spectra of the straight or bent germanium-coated nickel hollow waveguide.

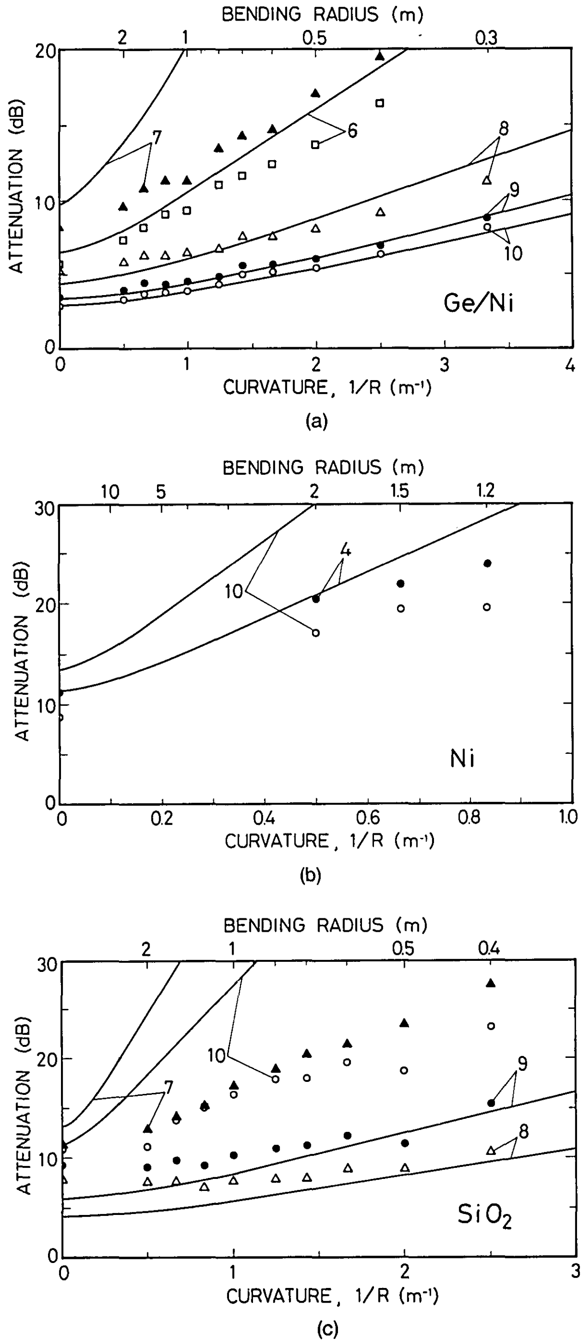

Fig. 5. Dependence of the attenuation on the curvature: (a) germanium-coated nickel waveguide, (b) nickel waveguide, (c) silica waveguide. The various characters indicate measured values, and solid curves indicate calculated values. The numbers indicate the wavelengths of light.

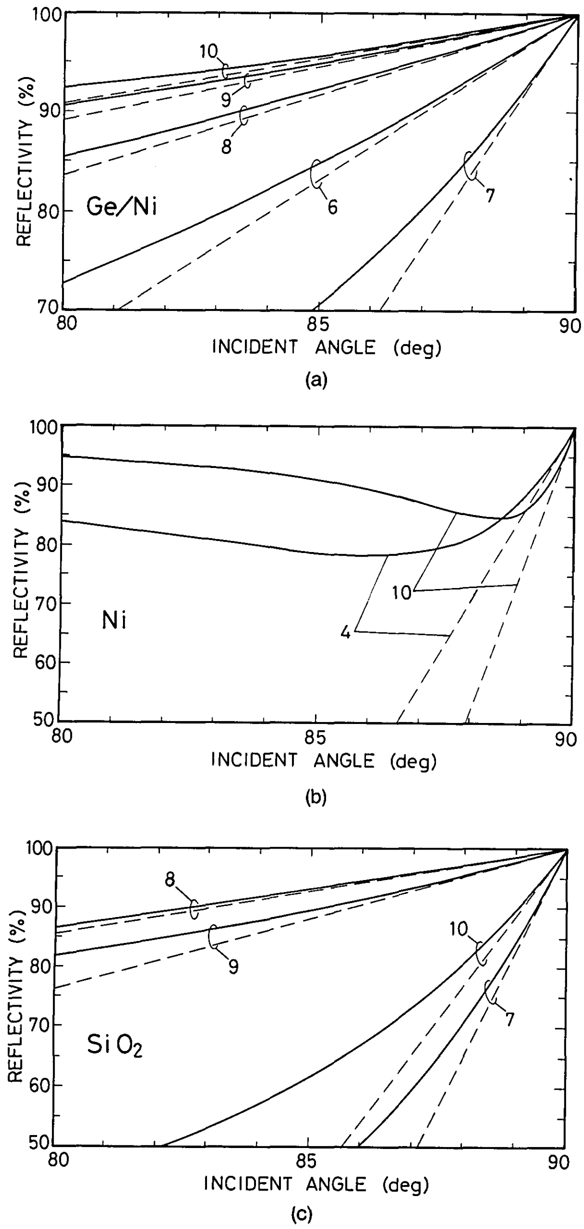

Fig. 6. Power reflectivity (solid curves) for various incident angles Ψ at these surfaces: (a) nickel with germanium film of 0.4-μm thickness, (b) uncoated nickel, (c) silica glass. Dashed curves are the asymptotes for the reflectivity curves. The numbers indicate the wavelengths.

considered in the ray-tracing method. However, Eq. (28) indicates that as far as the total loss is concerned, we should take into account only the directional angle θ_0 and need not care about the parameters r_0, ϕ_0, and φ_0. For a straight hollow waveguide, one of the authors proved that the total loss can be evaluated by considering only the meridional rays, since the losses of skew rays coincide with the loss of a corresponding meridional ray.[18] The present analysis indicates that the skewness need not be considered in the hollow waveguides even if they are bending.

It should be noted, however, that the above discussion cannot be applied to solid-core fibers. In those fibers rays of grazing incidence ($\Psi \simeq \pi/2$) suffer no loss on reflection at the boundary (total reflection), and hence Eqs. (14) and (15) do not hold. The conventional ray-tracing method would be necessary for solid-core fibers.[11]

Miyagi analyzed a bending loss in terms of electromagnetic theory and derived an expression

$$\alpha = \alpha_\infty[1 + (n_0 k_0 T/u_0)^4 (T/R)^2 \cdot \text{const.}], \tag{30}$$

where α_∞ denotes the attenuation constant in a straight waveguide.[10] Using the relation

$$u_0 = n_0 k_0 T \sin\theta_0 \fallingdotseq n_0 k_0 T \theta_0, \tag{31}$$

Eq. (30) reduces to

$$\alpha \fallingdotseq \alpha_\infty[1 + T^2/(R^2 \theta_0^{\,4}) \cdot \text{const.}]. \tag{32}$$

One should note a similarity between Eqs. (28) and (32).

Although the theoretical and experimental values coincide well with each other in low-loss wavelength regions, they differ greatly in high-loss regions. This discrepancy is related to the accuracy of approximation used in the calculation of reflectivity. In Fig. 6, the exact reflectivities at the waveguide walls are drawn with solid curves for various wavelengths. Dashed curves, which are calculated by Eq. (21), are the asymptotes for these curves. In the wavelength range of high reflectivity (e.g., 8–10 μm for germanium-coated nickel and 8–9 μm for silica glass), the asymptotes give good approximations at the angles of interest, i.e., $\Psi \simeq 87°$ to $\Psi = 90°$ ($\theta \simeq 0°$ to $\theta = 3°$). However, at the wavelengths of low reflectivity, the asymptotes deviate greatly from the exact curves. Consequently the calculated attenuation does not coincide with the measured attenuation in the high-loss wavelength region since large attenuation originates from the low reflectivity. Although more complicated calculation may enable the evaluation of high-loss waveguides, it would be of little use since such high-loss waveguides are not important from the practical point of view.

CONCLUSION

Bending losses of hollow waveguides have been analyzed in terms of geometrical optics. The present method is applicable to the incoherent light transmission and is simple compared with the conventional ray-tracing method. Numerically calculated optical losses coincide well with the measured ones in the low-loss wavelength regions of the waveguide, and hence the method is useful for the evaluation of bending losses.

ACKNOWLEDGMENT

This research was supported by a scientific research grant-in-aid (63850072) from the Ministry of Education, Science, and Culture of Japan.

REFERENCES

1. E. Garmire, T. McMahon, and M. Bass, "Flexible infrared waveguides for high-power transmission," IEEE J. Quantum Electron. **QE-16,** 23–32 (1980).
2. T. Hidaka, K. Kumada, J. Shimada, and T. Morikawa, "GeO_2–ZnO–K_2O glass as the cladding material of 940 cm^{-1} CO_2 laser light transmitting hollow-core waveguide," J. Appl. Phys. **53,** 5484–5490 (1982).
3. T. Miyashita and T. Manabe, "Infrared optical fibers," IEEE J. Quantum Electron. **QE-18,** 1432–1450 (1982).
4. M. Miyagi, A. Hongo, Y. Aizawa, and S. Kawakami, "Fabrica-

tion of germanium-coated nickel hollow waveguides for infrared transmission," Appl. Phys. Lett. **43**, 430–432 (1983).
5. R. M. Jenkins and R. W. J. Devereux, "Transmission characteristics of a curved hollow silica waveguide at 10.6 μm," IEEE J. Quantum Electron. **QE-22**, 718–722 (1986).
6. M. Saito, M. Takizawa, and M. Miyagi, "Optical and mechanical properties of infrared fibers," IEEE J. Lightwave Technol. **6**, 233–239 (1988).
7. E. A. Marcatili and R. A. Schmeltzer, "Hollow metallic and dielectric waveguides for long distance optical transmission and lasers," Bell Syst. Tech. J. **43**, 1783–1809 (1964).
8. E. Garmire, T. McMahon, and M. Bass, "Propagation of infrared light in flexible hollow waveguides," Appl. Opt. **15**, 145–150 (1976).
9. M. Miyagi, "Bending losses in hollow and dielectric tube leaky waveguides," Appl. Opt. **20**, 1221–1229 (1981).
10. M. Miyagi, K. Harada, and S. Kawakami, "Wave propagation and attenuation in the general class of circular hollow waveguides with uniform curvature," IEEE Trans. Microwave Theory Tech. **MTT-32**, 513–521 (1984).
11. C. Winkler, J. D. Love, and A. K. Ghatak, "Loss calculation in bent multimode optical waveguides," Opt. Quantum Electron. **11**, 173–183 (1979).
12. N. Croitoru, J. Dror, E. Goldenberg, D. Mendlovic, and S. Ruschin, "Use of metallic and dielectric films for hollow fibers," Fiber Integrated Opt. **6**, 347–361 (1987).
13. A. W. Snyder and D. J. Mitchell, "Bending losses of multimode optical fibers," Electron. Lett. **10**, 11–12 (1974).
14. C. Pask and A. W. Snyder, "Multimode optical fibers: interplay of absorption and radiation losses," Appl. Opt. **15**, 1295–1298 (1976).
15. Y. Matsuura, M. Saito, M. Miyagi, and A. Hongo, "Loss characteristics of circular hollow waveguides for incoherent infrared light," J. Opt. Soc. Am. A **6**, 423–427 (1989).
16. Y. Matsuura, M. Kawamura, M. Miyagi, and H. Ishikawa, "Spectral bending losses of incoherent IR light in various circular waveguides," Appl. Opt. **29**, 2214–2216 (1990).
17. E. D. Palik, *Handbook of Optical Constants of Solids* (Academic, Orlando, Fla., 1985), Part II.
18. M. Miyagi, "Waveguide-loss evaluation in circular hollow waveguides and its ray-optical treatment," IEEE J. Lightwave Technol. **LT-3**, 303–307 (1985).